Unusual nature of spin reorientation in $HoFeO_3$

G. P. Vorob'ev, A. M. Kadomtseva, I. B. Krynetkiĭ, and A. A. Mukhin

Moscow State University

(Submitted 7 September 1988)
Zh. Eksp. Teor. Fiz. **95**, 1049–1057 (March 1989)

The fine structure of the spin reorientation in holmium orthoferrite is investigated. Realization of a new canted phase $\Gamma_{12}(G_yG_zF_x)$ in $HoFeO_3$ is observed in the temperature interval 40–50 K. It is shown that the spin reorientation from the $\Gamma_4(G_xF_z)$ phase into $\Gamma_2(G_zF_x)$ is not through two phase transitions $\Gamma_4 \to \Gamma_{24} \to \Gamma_2$, as heretofore assumed, but in a more complicated manner, via three consecutive transitions $\Gamma_4 \to \Gamma_{24} \to \Gamma_{12} \to \Gamma_2$ at $T_1 \approx 60$ K, $T_2 \approx 50$ K, and $T_3 \approx 40$ K. Experimental and theoretical $H_x - T$ and $H_z - T$ diagrams are obtained and are in good agreement.

1. INTRODUCTION

It has been assumed until recently that the usual spin reorientation $\Gamma_4 \to \Gamma_{24} \to \Gamma_2$ ($G_xF_z \to G_xF_zG_zF_x \to G_zF_x$, **F** and **G** are the ferro- and antiferromagnetism vectors), which is most prevalent in orthoferrites, is observed in holmium orthoferrite at temperatures 50–60 K and is produced by a smooth rotation of the spins in the *ac* plane.[1–4] The onset of these transitions was attributed to the increase of the R–Fe exchange (R is a rare-earth element) of the Zeeman splitting of the lower doublet of Ho^{3+} ions in the Γ_2 phase ($2\Delta_{ex} = 9.8$ K) compared with the Γ_4 phase ($\Delta_{ex} = 0$ K).[2–4] It is known, however, that in $HoFeO_3$, just as in $DyFeO_3$, conditions exist favoring spin reorientation into an antiferromagnetic phase Γ_1 (G_y) that stabilizes the magnetic anisotropy via the Van Vleck mechanism connected with the lowering of the ground-doublet energy centers of the ions Ho^{3+} and Dy^{3+} through interaction with the excited levels.[4] It is just this mechanism which leads to the appearance in $DyFeO_3$ of a spontaneous spin reorientation (SSR) of the Morin type, $\Gamma_4 \to \Gamma_1$ ($G_xF_z \to G_y$) at $T = 40$ K. It was shown in Ref. 5 that SSR of the Morin type is observed also in the compound $Ho_{0.5}Dy_{0.5}FeO_3$ at $T = 45$ K. Since replacement of Dy^{3+} ions by Ho^{3+} ions changes the Morin temperature insignificantly, it is natural to assume that in pure $HoFeO_3$ the Van Vleck mechanism which stabilizes the $\Gamma_1(G_y)$ configuration should make an appreciable contribution to the anisotropy energy. This is also directly attested to by investigations of the dynamic properties of $HoFeO_3$.[6–8]

Whether the above tendency leads in $HoFeO_3$ to a real transition into the antiferromagnetic state $\Gamma_1(G_y)$ via the Van-Vleck mechanism, however, calls for additional experimental research, which is the subject of the present paper.

2. EXPERIMENTAL RESULTS

We measured the temperature dependences of the nonmagnetic properties (thermal expansion, Young's modulus, internal friction), and also the magnetization and magnetostriction isotherms, of $HoFeO_3$ single crystals grown from a molten solution of lead compounds, in fields up to 60 kOe and at temperatures covering the spin-reorientation region. The magnetic-measurement results were used to plot the temperature dependences of the spontaneous magnetic moments m_x and m_z along the crystal axes $a(x)$ and $c(z)$ (Fig. 1). It is seen from this figure that a spin reorientation $\Gamma_4(G_xF_z) \to \Gamma_2(G_zF_x)$ occurs below $T_1 = 60$ K, and the magnetic moment along the c axis vanishes at $T_2 = 50 \pm 2$ K. No anomalies pointing to a complicated character of the SRT were observed in $m_x(T)$. Additional information on the SRT anomalies in $HoFeO_3$ was obtained by analysis of the temperature dependence of the non-magnetic characteristics. Bends were observed in the temperature dependence of the thermal expansion (Fig. 2a) not only at $T_1 = 60$ K and $T_2 = 50$ K, but also at 40 K. This may indicate a change in the magnetic structure for spin reorientation in a wider temperature range than obtained from magnetic measurements. The temperature dependence of Young's modulus E_c along the c axis (Fig. 2b) revealed, besides the strong decrease of this modulus in the temperature interval 50–60 K as a result of the canted magnetic structure, also a small "dip" in the $E_c(T)$ plot, attesting to the absence of the "rigid" magnetic structure $\Gamma_2(G_zF_x)$ also in the temperature interval 40–50 K.

In the same temperature interval we have observed also a noticeable internal-friction (Fig. 2b) increase that stems apparently from the irreversible energy loss due to spin rotation. Since the magnetization along the c axis is zero in the interval 40–50 K (see Fig. 1), it can be assumed that the small decrease of Young's modulus at these temperatures can be due to the presence of the canted magnetic structure Γ_{12}, but this requires a more rigorous proof. The validity of the assumed interpretation of the anomalies of the $HoFeO_3$ structure in the SRT region was confirmed by a study of orientational transitions induced by a magnetic field.

One of the most effective ways of investigating orientational transitions is to study the magnetostriction λ_c produced along the c axis by spin reorientation. We have investi-

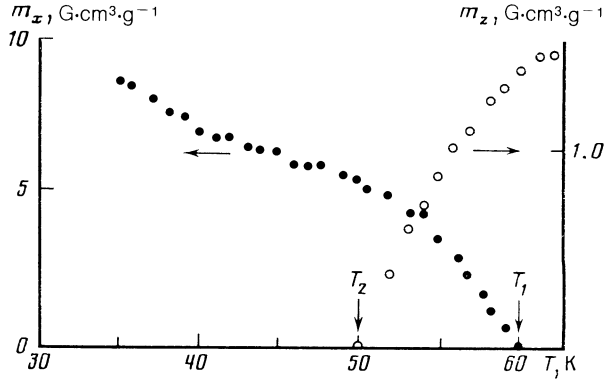

FIG. 1. Temperature dependence of the spontaneous magnetic moments m_x and m_z along the a and c axes of an $HoFeO_3$ crystal.

 0038-5646/89/030604-05$04.00

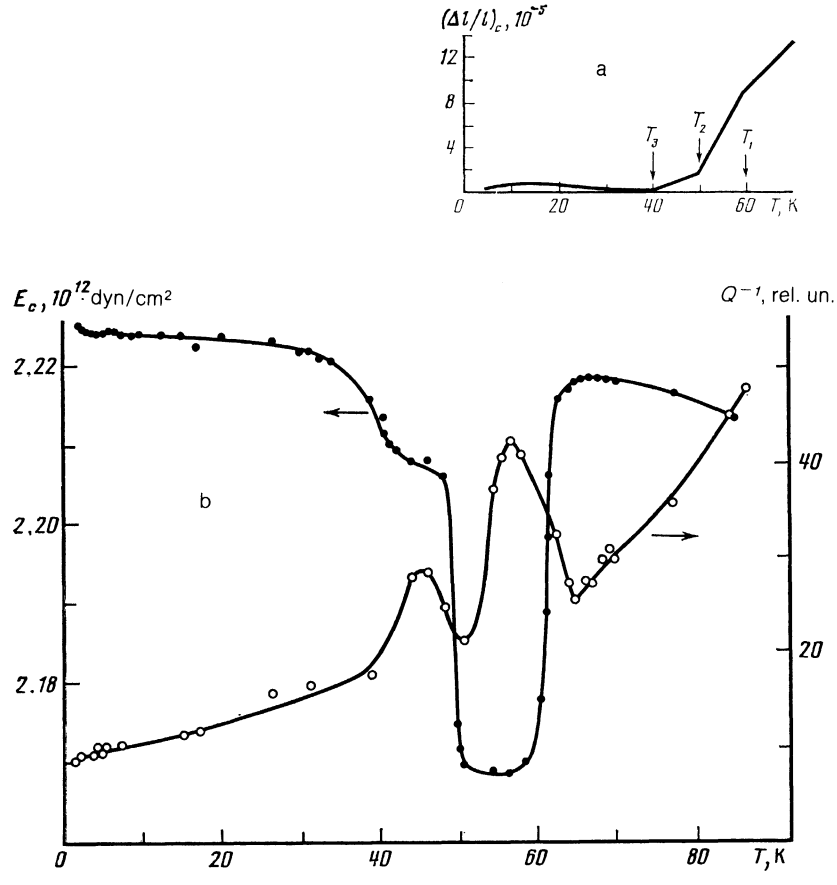

FIG. 2. Temperature dependences: a) of the thermal expansion and b) of the Young's modulus E_c and the internal friction Q^{-1} of an $HoFeO_3$ crystal.

gated the field dependences of the magnetostriction for spin reorientation induced by a magnetic field $\mathbf{H}\|\mathbf{z}$ or $\mathbf{H}\|\mathbf{x}$ (Fig. 3). For $\mathbf{H}\|\mathbf{z}$ the magnetostriction at temperatures $T > T_1 = 60$ K is practically zero (curve 1 of Fig. 3), since the magnetic structure $\Gamma_4(G_xF_z)$ observed at these temperatures is stable to field orientation along the c axis. In the temperature interval 50–60 K application of a field along the

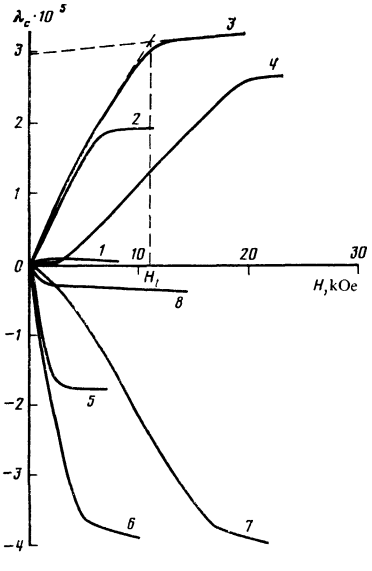

FIG. 3. Field dependences of the magnetostriction of $HoFeO_3$ at $\mathbf{H}\|\mathbf{z}$, (1—59.5 K, 2—54.6 K, 3—52.2 K, 4—48 K) and at $\mathbf{H}\|\mathbf{x}$ (5—52.6 K, 6—62 K, 7—83.3 K, 8—45 K).

c axis causes an orientation transition $\Gamma_{24} \rightarrow \Gamma_4$ accompanied by the onset of magnetostriction. The growth of the magnetostriction ceases on reaching the threshold field H_t in which the spin reorientation is completed, in which case bends appear on the magnetostriction isotherms (curves 2 and 3 of Fig. 3). The threshold field was determined from the intersection of the tangents to the sections of the $\lambda_c(H)$ plot in the region of the bend, as shown by curve 3 of Fig. 3. Negative magnetostriction is similarly produced at $\mathbf{H}\|\mathbf{x}$, corresponding to the $\Gamma_{24} \rightarrow \Gamma_2$ STR in the temperature range $50 < T < 60$ K (curve 5 of Fig. 3) and to the transition $\Gamma_4 \rightarrow \Gamma_2$ at $T > 60$ K (curves 6 and 7 of Fig. 3). A bend is also observed on the magnetostriction isotherms at H_t, followed by cessation of the magnetostriction growth and by an increase of the field.

Figure 4 shows the temperature dependence of the maximum magnetostriction corresponding to the completion of the spin reorientation at $\mathbf{H}\|\mathbf{z}$ and $\mathbf{H}\|\mathbf{x}$ and obtained from the λ_c curves (Fig. 3) by extrapolation to zero field, while Figs. 5a and 5b show the corresponding $H_x(T)$ and $H_z(T)$ plots. It is important, as seen from Figs. 3 (curves 4 and 7) and 4, that the magnetostriction at $\mathbf{H}\|\mathbf{z}$ and $\mathbf{H}\|\mathbf{x}$ differs from zero also in the temperature interval 40–50 K, attesting to the complicated character of the SRT in $HoFeO_3$. Thus, magnetostriction can occur for $\mathbf{H}\|\mathbf{x}$ at temperatures $40 < T < 50$ K (curve 8 of Fig. 3) only if the magnetic moment is deflected from the a axis of the crystal, i.e., the magnetic structure at these temperatures is not Γ_2. The deflection of the magnetic moment from a axis is apparently small, since the magnetostriction (curve 2 of Fig. 4) and the threshold field (Fig. 5a)

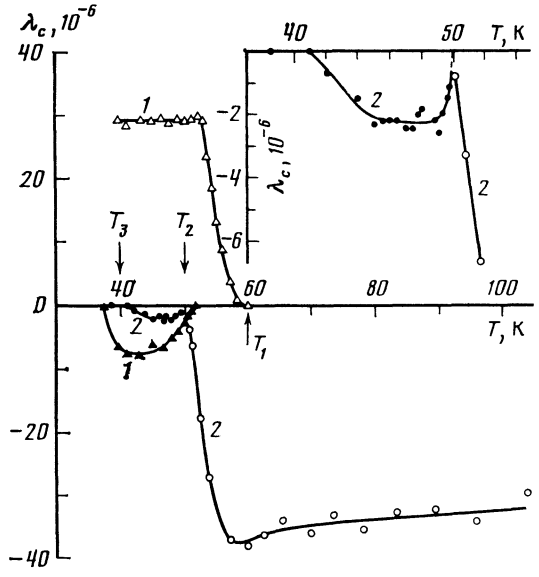

FIG. 4. Temperature dependence of magnetostriction along the c axis of the $HoFeO_3$ crystal: 1—$\mathbf{H}\|\mathbf{z}$, (▲—$\Gamma_{124}\rightarrow\Gamma_{24}$, △—$\Gamma_{24}\rightarrow\Gamma_4$ transition), 2—$\mathbf{H}\|\mathbf{x}$ (●—$\Gamma_{12}\rightarrow\Gamma_2$, ○—$\Gamma_{24}\rightarrow\Gamma_2$).

are smaller by almost an order of magnitude than those observed at $T > 50$ K. Recognizing that at these temperatures the component of the magnetic moment along the c axis is zero, it can be concluded that a $\Gamma_{12}(G_yG_zF_x)$ magnetic structure is present below 50 K.

Since a Γ_{24} magnetic structure is observed at $T > 50$ K, it is natural to conclude that in the absence of a magnetic field an unusual orientational $\Gamma_{24}\rightarrow\Gamma_{12}$ transition is realized at $T = 50 \pm 2$ K. When the temperature is decreased below T_2, the magnetostriction and the threshold field decrease continuously and vanish at $T_3 = 40 \pm 2$ K, which attests to completion of the spin reorientation in the bc plane ($\Gamma_{12}\rightarrow\Gamma_2$ transition). A complicated spin reorientation at temperatures $40 < T < 50$ K was observed also for $\mathbf{H}\|\mathbf{z}$. The presence of two bends on the plot of the magnetostriction field dependence (curve 4 of Fig. 3) can be explained by assuming that $\mathbf{H}\|\mathbf{z}$ induces in succession two types of reorientation transitions, namely, $\Gamma_{124}\rightarrow\Gamma_4$ accompanied by negative magnetostriction and $\Gamma_{24}\rightarrow\Gamma_4$ with positive magnetostriction. The temperature dependences of the magnetostriction corresponding to these phase transitions, and the H_x–T and H_z–T diagrams are shown in the insets of Figs. 4 and 5.

3. THEORY AND DISCUSSION OF RESULTS

As already noted in the Introduction, of principal importance for the explanation of the mechanisms governing the observed orientational phase transitions in $HoFeO_3$ is allowance for the anisotropy of the Ho–Fe exchange interaction. The quasidoublet structure[9] of the spectrum of the Ho^{3+} ion in the crystal field leads to: a) anisotropy of the exchange splitting ($2\Delta_{1\eta}$) of the ground quasidoublet of the Ho^{3+} ion, and b) anisotropy of the shift $\Delta E_{VV}{}^{(1)}$ of its centroid by the mixing of the excited states via R–Fe interaction (analog of Van Vleck paramagnetism). As a result, the energy levels of the Ho^{3+} ground quasidoublet in the crystal, exchange, and external fields can be represented by[4,10]

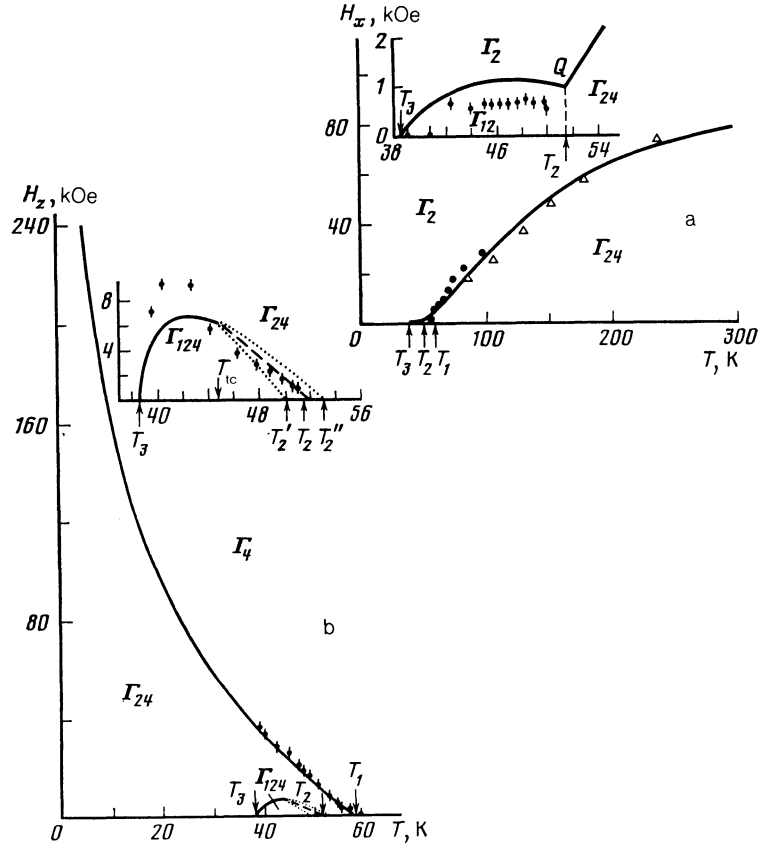

FIG. 5. Phase diagrams: a) H_x–T, b) H_z–T. Points—experiment (●—present paper, △—Ref. 15), lines—theory (solid—second-order PT, dashed—first-order PT, dotted—stability-loss lines). T_{tc}— temperature corresponding to tricritical points; T_2', T_2''—stability-loss points of the phases Γ_{24} and Γ_{12} respectively and for $H_z = 0$.

$$E_{1\eta}^{\pm}=\pm\Delta_{1\eta}+\Delta E_{VV}^{(1)}, \quad (1)$$

where

$$\Delta_{1\eta}^2=\Delta_{cf}^2+[BG_z+\mu_\eta(\mathbf{H}+a\mathbf{F})]^2, \quad (2)$$

Δ_{cf} is half the splitting in the crystal field, a and B are respectively the isotropic and anisotropic R–Fe exchange constants, $\mu_\eta \equiv \mu_\pm = (\mu_x, \pm\mu_y, 0)$ is the magnetic moment of the quasidoublet, and the subscript $\eta = \pm$ distinguishes between two crystallographic nonequivalent positions. We represent the quantity $\Delta E_{VV}^{(1)}(\mathbf{G})$, calculated in second order perturbation theory in the R–Fe exchange interaction, in the form

$$\Delta E_{VV}^{(1)}(\mathbf{G})=\text{const}+\Delta E_{ac}^{(1)}G_z^2+\Delta E_{ab}^{(1)}G_y^2, \quad (3)$$

where we regard the coefficients $\Delta E_{ac,ab}^{(1)}$ as phenomenological parameters. Note that allowance for the Van Vleck contribution to the Ho^{3+} energy is of fundamental importance, since $\Delta E_{VV}^{(1)}$, in contrast to $\Delta_{1\eta}$, contributes to the anisotropy energy not only in the *ac* plane, but also in the *ab* plane, a circumstance essential for explaining the phase transformations in $HoFeO_3$. The energy levels of the excited quasidoublets of Ho^{3+} are also similar to (1)–(3), if it is assumed that their wave functions in the crystal field (C_s symmetry) pertain, just as for the ground quasidoublet, to different representations of the C_s group.

In the high-temperature approximation ($\Delta_{1\eta} \ll T$) the $HoFeO_3$ nonequilibrium thermodynamic potential can be written (after minimization with respect to $\mathbf{F}$) in the form[10]

$$\Phi(G)=\tfrac{1}{2}K_{ac}G_z^2+\tfrac{1}{2}K_{ab}G_y^2+\tfrac{1}{4}K_2G_z^4+\tfrac{1}{4}K_2'G_y^4$$
$$+\tfrac{1}{2}K_2''G_y^2G_z^2-m_xH_xG_z-m_zH_zG_x-\tfrac{1}{2}\sum_\alpha \chi_\perp^\alpha H_\alpha^2$$
$$+\tfrac{1}{2}\sum_{\alpha,\beta}\Delta\chi^{\alpha\beta}H_\alpha H_\beta G_\alpha G_\beta-\tfrac{1}{2}\sum_\alpha(\chi_R^\alpha+\chi_{VV}^\alpha)H_\alpha^2, \quad (4)$$

where

$$m_x=m_x^0+N\mu_x\Delta_{ex}^0/(T+\Theta_x), \quad m_{x,z}^0=m_{x,z}^{Fe}+m_{x,z}^{VV}, \quad m_z=m_z^0, \quad (5)$$

$$\chi_\perp^\alpha=\chi_\perp^{Fe}(1+\eta_\alpha)^2, \quad \Delta\chi^{\alpha\beta}=(\chi_\perp^{Fe}-\chi_\parallel^{Fe})(1+\eta_\alpha)(1+\eta_\beta),$$

$$\eta_\alpha=\chi_R^\alpha a/M_0^{Fe},$$

$$\chi_R^{x,y}=N\mu_{x,y}^2/(T+\Theta_{x,y}), \quad \chi_R^z=0, \quad \Delta_{ex}^0=B+a\mu_xF_0,$$

$$F_0=d/A,$$

$$K_{ac}=K_{ac}^0-N(\Delta_{ex}^0)^2/(T+\Theta_x), \quad K_{ac}^0=K_{ac}^{Fe}+K_{ac}^{VV},$$

$$K_{ab}=K_{ab}^{Fe}+K_{ab}^{VV},$$

N is the number of Ho^{3+} ions per gram, and A and d are respectively the isotropic and antisymmetric Fe–Fe exchange. In the derivation of (4) we have taken into account the R–R interaction determined by the paramagnetic Curie temperatures $\Theta_{x,y}$, and also the inequalities $M_0^{Fe}a/A \ll 1$ and $N(a\mu_x)^2/A\Theta_x \ll 1$ ($M_0^{Fe}=5\mu_BN$), which are valid for orthoferrites.

Among the Van Vleck contributions to the thermodynamic potential (4), the most important role is played in our case by the renormalization of the anisotropy constant K_{ab} in the *ab* plane on account of K_{ab}^{VV} and its temperature dependence. Taking into account the temperature population of the excited states of the Ho^{3+} ion, we can express $K_{ab}^{VV}(T)$ in the form (by analogy with Refs. 8 and 10)

$$K_{ab}^{VV}(T)=2\sum_i \Delta E_{ab}^{(i)}\exp\left(-\frac{E_i}{T}\right)\Big/\sum_i \exp\left(-\frac{E_i}{T}\right),$$

where E_i is the energy of the center of gravity of the ground ($i=1$) and excited ($i\geqslant 2$) quasidoublets of the Ho^{3+} ion in the crystal field, while $\Delta E_{ab}^{(i)}$ is their displacement when $\mathbf{G}$ is rotated from the *b* to the *a* axis ($\Delta E_{ab}^{(i)} \ll E_i$). A similar expression holds also for $K_{ac}^{VV}(T)$ with $\Delta E_{ab}^{(i)}$ replaced by $\Delta E_{ac}^{(i)}$.

We consider first on the basis of (4) the spontaneous phase transitions (PT). According to the above experimental data as well as the data of Ref. 8 spin reorientation from the phase Γ_4 and Γ_2 occurs first in the *ac* plane ($\Gamma_4 \to \Gamma_{24}$) and next in the *bc* plane ($\Gamma_{12} \to \Gamma_2$). The $\Gamma_4 \to \Gamma_{24}$ transition takes place if $K_{ac}(T_1)=0$, and the $\Gamma_{12} \to \Gamma_2$ transition if $K_{cb}(T_3)=K_{ab}(T_3)-K_{ac}(T_3)-K_2+K_2''=0$. Obviously, to meet the last condition K_{ab} must be appreciably decreased, and this is accomplished by the negative Van Vleck contribution to K_{ab}. Since both transitions are of second order, this imposes on the fourth-order anisotropy constants in the planes *ac* and *bc* the respective conditions $K_2>0$ and $\tilde{K}_2=K_2+K_2'-2K_2''>0$. As to the reorientation from the *ac* plane into the *bc* plane ($\Gamma_{24} \to \Gamma_{12}$), it follows from an analysis of $\Phi(\mathbf{G})$ that it can be effected either jumpwise or continuously (i.e., via two second-order PT; $\Gamma_{24} \to \Gamma_{124} \to \Gamma_{12}$), depending on the ratio of the constants K_2, K_2' and K_2''. For $HoFeO_3$ we prefer the first variant, which corresponds to the conditions $K_2>0$ and $\tilde{K}_2>0$, while for $DyFeO_3$, judging from the data of Ref. 4, we prefer the condition $K_2'<0$.[1)]

The angles that determine the orientation of the vector $\mathbf{G}$ relative to the *c* axis ($G_z=\cos\theta$) in the planes *ac* (Γ_{24} phase) and *bc* (Γ_{12} phase) are given by

$$\cos^2\theta_1=-K_{ac}/K_2, \quad \cos^2\theta_2=1+K_{cb}/\tilde{K}_2.$$

From an analysis of the behavior of the magnetostriction (see Fig. 4) connected with the rotation of the vector $\mathbf{G}(\lambda_c=\lambda_1G_x^2+\lambda_2G_y^2)$ it follows that the rotation of $\mathbf{G}$ in the *ac* plane in the interval T_1-T_2 amounts to practically 90°, as evidenced by the appreciable changes of λ_c in this interval. No complete reorientation of $\mathbf{G}$ to the *c* axis takes place at the point T_2, for in this case λ_c remains constant (see the inset of Fig. 4). In the other reorientation interval (T_2-T_3) the small magnetostriction of the $\Gamma_{12} \to \Gamma_2$ transition indicates that the angle of deviation of $\mathbf{G}$ from the *c* axis in the *bc* plane is not large. Its maximum can be estimated, from curve 2 of Fig. 4, at $\theta_2 \approx 15$–$20°$ under the assumption $\lambda_2 \sim \lambda_1$, where $\lambda_1 \approx (3$–$4)\cdot 10^{-5}$.

We consider now the magnetic-field-induced orientational transitions.

$\mathbf{H}\|\mathbf{x}$. In this case the magnetic field induces two second-order PT, $\Gamma_{24} \to \Gamma_2$ and $\Gamma_{12} \to \Gamma_2$, and a first-order PT $\Gamma_{24} \to \Gamma_{12}$; their lines on the H_x–T plane are determined by the following equations obtained from (4):

$$\Gamma_{24} \to \Gamma_2: \quad \Delta\chi^{xx}H_x^2+m_xH_x-(K_{ac}+K_2)=0, \quad (6)$$

$$\Gamma_{12} \to \Gamma_2: \quad m_xH_x+K_{cb}=0, \quad (7)$$

$$\Gamma_{24}\to\Gamma_{12}:\ (\Delta\chi^{xx}H_x^2+m_xH_x-K_{ac}-K_2)^2(\bar{K}_2+m_xH_x/2)$$
$$=(m_xH_x+K_{cb})^2(K_2+m_xH_x/2). \quad (8)$$

In the derivation of (8) we have taken it into account that in the PT $\Gamma_{12}\to\Gamma_{24}$ the deviation angles of **G** from the *c* axis are small.

Figure 5a shows the numerically computed H_x-T phase diagram of $HoFeO_3$, which agrees well with experiment. Its characteristic feature is the presence of a bicritical point Q at which two second-order PT lines, $\Gamma_{12}\to\Gamma_2$ and $\Gamma_{24}\to\Gamma_2$, and a first-order PT $\Gamma_{24}\to\Gamma_{12}$ converge.[2)] The coordinates of these points are given by the equations

$$\Delta\chi^{xx}H_x^2=K_{ab}+K_2''=\Delta\chi^{xx}K_{cb}^2/m_x^2.$$

The phase diagram was numerically computed for the following values of the thermodynamic potential (4), which were determined in Ref. 8 from an analysis of the independent dynamic magnetic properties of $HoFeO_3$:

$\Delta_{ex}^0=4.7$ K, $\Theta_x=3$ K, $a=-80$ kOe,

$\mu_x=3.25\mu_B$, $m_x^0=0.0385\mu_B$,

$\chi_\perp^{Fe}=0.65\cdot10^{-5}$ cm^3/g $F_0=0.75\cdot10^{-2}$,

$K_{ac}^{Fe}+2\Delta E_{ac}^{(1)}=0.3$ K,

$\Delta E_{ac}^{(2)}=0.36$ K, $\Delta E_{ac}^{(3)}=-0.3$ K,

$K_{ab}^{Fe}+2\Delta E_{ab}^{(1)}=-0.173$ K,

$\Delta E_{ab}^{(2)}=1.35$ K, $\Delta E_{ab}^{(3)}=0.6$ K,

$K_2\approx-K_2''=0.07$ K, $K_2'=-0.12$ K.

The energies of the first and second quasidoublets of the Ho^{3+} ions in crystal fields were assumed to be $E_1=0$ and $E_2=120$ K (Ref. 9); and the others were taken into account by introducing their centroid with energy $E_3=300$ K (Ref. 8).

H||z. In this field there is induced at $T<T_1$ a second-order PT $\Gamma_{24}\to\Gamma_4$, which takes place on a line defined by the equation

$$\Delta\chi^{zz}H_z^2+m_zH_z+K_{ac}=0, \quad (9)$$

and the PT $\Gamma_{124}\to\Gamma_{24}$ in the interval T_2-T_3. The latter has a variable character. At $T_3<T<T_{tc}$ it is realized as a second-order PT on a line defined by the equation

$$m_zH_z=-(K_{ab}+K_2''\cos^2\theta_0)\sin\theta_0, \quad (10)$$

where

$$\cos^2\theta_0=(K_{ab}-\bar{K}_{ac})/(K_2-K_2''),\quad \bar{K}_{ac}=K_{ac}+\Delta\chi^{zz}H_z^2, \quad (11)$$

and θ_0 is an angle that determines the orientation of **G** in the *ac* plane on the line of this PT. Above the tricritical-point temperature (T_{tc}), the PT $\Gamma_{124}\to\Gamma_{24}$ is of first order. The tricritical-point coordinates are determined by Eqs. (10) and (11), with

$$\sin^2\theta_0[(2K_2+K_2'')(2K_2'+K_2'')-9(K_2'')^2]=2(K_{ab}+K_2'')\bar{K}_2. \quad (12)$$

The equations for the remaining lines of the phase diagrams are unwieldy and are left out. Figure 5b shows the H_z-T phase diagram of $HoFeO_3$ computed for $m_z=0.07\mu_B$ and for the cited data of Ref. 8. On the whole, this diagram agrees well with our experiment.

4. CONCLUSION

Our comprehensive investigations of the magnetic and magnetoelastic properties as well as of the nonmagnetic characteristics of $HoFeO_2$ have shown that in the temperature interval 40–50 K there is realized in $HoFeO_3$ a new canted phase $\Gamma_{12}(G_yG_zF_x)$ in which the antiferromagnetism vector **g** is deflected by a small angle (15–20°) from the *c* axis in the *bc* plane. This has allowed us to conclude that the spin reorientation from the Γ_4 phase into the Γ_2 phase of $HoFeO_3$ proceeds not via two second-order phase transitions, $\Gamma_4\to\Gamma_{24}\to\Gamma_2$, as heretofore assumed, but in a more complicated manner: a $\Gamma_4\to\Gamma_{24}$ PT takes place at $T_1\approx60$ K, a $\Gamma_{24}\to\Gamma_{12}$ transition at $T_2\approx50$ K, and a $\Gamma_{12}\to\Gamma_2$ transition at $T_3\approx40$ K. We have shown that the cause of the transitions to the new canted phase Γ_{12} is the appreciable Van Vleck contribution to the anisotropy energy, due to the displacement of the center of gravity of the ground quasidoublet of the Ho^{3+} ion on account of interaction with the excited states. Experimental and theoretical H_x-T and H_z-T phase diagrams have been obtained and are in good agreement with one another. We note also that our qualitative conclusions and quantitative results agree well with results of independent investigations of the dynamic magnetic properties of $HoFeO_3$ (Ref. 8), which were used by us to compute the phase diagrams.

[1)]For the continuous reorientation $\Gamma_{12}\to\Gamma_{124}\to\Gamma_{24}$ it is necessary to meet the conditions $K_2,K_2'>0$ and $K_2K_2'>(K_2'')^2$ (see also Ref. 11).

[2)]A similar point exists also on the H_x-T diagrams of $DyFeO_3$ (Refs. 12 and 13) and $DyFe_{1-x}Al_xO_3$ (Ref. 14).

[1]A. Apostolov and J. Sivardiere, Comp. Rend. B268, 208 (1969).
[2]R. L. White, J. Appl. Phys. **40**, 1061 (1969).
[3]J. C. Walling and R. L. White, Phys. Rev. **B10**, 4748 (1974).
[4]K. P. Belov, A. K. Zvezdin, A. M. Kadomtseva, and R. Z. Levitin, *Orientational Transitions in Rare-Earth Magnets* [in Russian], Nauka, 1979.
[5]K. P. Belov, A. K. Zvezdin, A. M. Kadomtseva, *et al.*, Zh. Eksp. Teor. Fiz. **68**, 743 (1975) [Sov. Phys. JETP **41**, 369 (1975)].
[6]A. M. Balbashov, G. V. Kozlov, S. P. Lebedev, *et al.*, Pis'ma Zh. Eksp. Teor. Fiz. **43**, 33 (1986) [JETP Lett. **43**, 41 (1986)].
[7]G. V. Kozlov, S. P. Lebedev, A. A. Mukhin, *et al.*, Abstracts, 24th All-Union Conf. on Low-Temp. Phys., Tbilisi, 1986, Part III, p. 28.
[8]A. M. Balbashov, G. V. Kozlov, S. P. Lebedev, *et al.*, Preprint No. 97, Inst. Gen. Phys. USSR Acad. Sci, 1988. Kratk. Soobshch. Fiz. No. 9, 21 (1988). Zh. Eksp. Teor. Fiz. **95**, 1092 (1989) [Sov. Phys. JETP **68**, (1989) (this issue)].
[9]H. Schuchert, S. Hufner, and R. Faulhaber, Z. Phy. **B220**, 280 (1969).
[10]A. K. Zvezdin, M. V. Matveev, A. A. Mukhin, and A. A. Popov, *Rare-Earth Ions in Magnetically Ordered Crystals* [in Russian], Nauka, 1985.
[11]A. P. Agafonov and A. S. Moskvin, Fiz. Tverd. Tela (Leningrad) **30**, 612 (1988) [Sov. Phys. Solid State **30**, 353 (1988)].
[12]V. V. Erimenko, S. L. Gnatchenko, N. F. Kharchenko, *et al.*, Europhys. Lett. **11**, 1327 (1987).
[13]P. Yu. Marchukov and E. G. Rudashevskiĭ, Kratk. Soobshch. Fiz. No. 7, 53 (1987).
[14]V. N. Derkachenko, A. K. Zvezdin, A. M. Kadomtseva, *et al.*, Abstracts, 21st All-Union Conf. on Low Temp. Phys., Khar'kov, 1980, Part II, p. 159.
[15]V. A. Semenov, Author's Abstract of Candidate's Dissertation, Moscow State Univ., 1985.

Translated by J. G. Adashko